Behavior of relative state selective photoionization cross sections of RbBr molecules in the valence region

A. Karpenko,[1,*] D. Iablonskyi,[1,2] S. Urpelainen,[1,3] and H. Aksela[1]

[1]*Department of Physical Sciences, University of Oulu, Box 3000, FI-90014 Oulu, Finland*

[2]*Institute of Multidisciplinary Research for Advanced Materials, Tohoku University, Sendai 980-8577, Japan*

[3]*MAX IV Laboratory, Lund University, Box 118, SE-22100 Lund, Sweden*

(Received 28 July 2014; published 8 December 2014)

The photon energy dependence of relative photoionization cross sections in the valence ionization energy region of 5 to 45 eV for $4p$ and $4s$ orbitals of Rb and Br ions in RbBr vapors has been investigated. The behavior of state selective cross sections of molecular valence orbitals has been analyzed by comparing the observed $4p$ to $4s$ photoelectron intensity branching ratios with atomic state selective photoionization cross sections of Kr, taking into account the mixing between Br $4s^{-1}$ and Rb $4p^{-1}$ molecular states. Using atomic dipole matrix elements to calculate the photoionization intensity of alkali halides has been suggested.

DOI: 10.1103/PhysRevA.90.062505 PACS number(s): 33.60.+q, 31.15.A−

I. INTRODUCTION

Alkali halides are typically considered to be molecules exhibiting ionic bonding, in which the ionic character increases as the atomic number of alkali-metal and halogen atoms increases. Assuming completely ionic bonding, RbBr can be considered to be made of Br^- and Rb^+ ions, which are isoelectronic with Kr.

Photoionization of outer-shell electrons in noble-gas atoms has served as a benchmark for experimental and theoretical methods over the last few decades [1–3]. Recently, Caló *et al.* [4] investigated the Kr valence photoelectron satellite lines in the photon energy region below the $3d$ ionization threshold. Strong photon energy dependence was found in the experimental cross sections of the satellite lines.

Photoionization cross sections (PCS) are among those fundamental quantities which provide direct insight into the electronic structure of atoms, molecules, and solids. They give the total ionization probability of the system by electromagnetic radiation of a given energy. A more specific and informative quantity for subshell-dependent ionization behavior is the state-selective PCS, given by

$$\sigma_{if}(h\nu) = \frac{4a_0^2\pi^2\alpha}{3} h\nu |M_{if}|^2, \tag{1}$$

where α is the fine-structure constant, a_0 is the Bohr radius, and $h\nu$ is the photon energy in Rydberg units. The matrix element M_{if} describes, in the dipole approximation, the dipole transition between the initial state i and the final state f:

$$|M_{if}|^2 = \left| \langle f | \sum_\mu r_\mu | i \rangle \right|^2, \tag{2}$$

with $\sum_\mu r_\mu$ being the dipole operator of the n-electron system.

Benzaid *et al.* [5] reported a comprehensive experimental study of the partial photoionization cross sections of atomic Br across the entire autoionization regime extending from the first ionization threshold $Br^+(^3P_2)$ to the highest threshold $Br^+(^1S_0)$. The autoionization decay patterns arising from the $4p \rightarrow ns,md$ excitations were discussed. Lin and Saha [6] calculated the partial photoionization cross sections for the outer p subshell of the ground state of atomic Br. The calculated energy positions for the autoionizing resonances $4p^4(^1D)md$, $4p^4(^1D)ns$, $4p^4(^1S)md$, and $4p^4(^1S)ns$ were found to be in good agreement with experimental measurements.

Recently, Karpenko *et al.* [7,8] showed that the third-order algebraic diagrammatic construction (ADC) method [9,10] implemented in the DIRAC10 program [11] is capable of reproducing valence and inner-valence photoelectron spectra (PES) of alkali bromide molecules. The binding energies and ionization strengths for the $4p$ and $4s$ orbitals of Br^-, $2p$ orbital of Na^+, $3p$ and $3s$ orbitals of K^+, and $4p$ and $4s$ orbitals of Rb^+ were calculated [7] using this method.

Despite the fact that the ionization energies of systems exhibiting ionic bonding, such as alkali halide molecules, can be reproduced well by *ab initio* methods, an accurate prediction of spectral intensities remains a challenging task. A full comparison of spectral intensities between theory and experiment is usually not possible since the calculated intensity distribution is based on the occupation of orbitals, and the actual values of transition dipole matrix elements M_{if} are left out. Dipole matrix elements for noble gases may serve as a starting point for future development of the theory.

In this work, the behavior of valence photoionization cross sections of the RbBr monomer has been studied by comparing the observations to atomic Kr. The spectral intensities of $4s^{-1}$ and $4p^{-1}$ features of Br and Rb ions [8] in the RbBr molecule were measured as a function of photon energy. Branching ratios of the valence photoelectron $4p/4s$ lines were then extracted for each ion. The difference between the observed $4p/4s$ branching ratios of Rb^+ and Br^- was explained using the newly developed model based on photoionization cross sections of atomic Kr accounting for the mixing between Br $4s^{-1}$ and Rb $4p^{-1}$ states.

II. EXPERIMENT

The measurements were carried out at the undulator beam line I411 [12] of the MAX-II storage ring in Lund, Sweden.

The RbBr vapor beam was generated using an inductively heated oven with a stainless steel crucible [13] containing

*oleksandr.karpenko@oulu.fi

the sample. The sample was heated to 360 °C. The temperature was monitored using a thermocouple connected to the crucible. The photoelectrons were detected using a Scienta R4000 hemispherical electron analyzer placed at the "magic" emission angle of 54.7° with respect to the electric-field vector of the linearly polarized synchrotron radiation.

The electron binding energy calibration was performed by introducing Kr gas into the experimental chamber and recording the well-known [14] Kr $4p_{3/2}$ (14.00 eV) and $4p_{1/2}$ (14.67 eV) photoelectron lines simultaneously with the RbBr PES. The photon energies between 40 and 120 eV were used in the measurements. The PES were recorded with 100 eV pass energy of the electron spectrometer. Total instrumental broadening due to the photon bandwidth and the analyzer contribution is represented by Gaussian distribution with a FWHM estimated at 130 meV.

The spectral intensities were corrected for the changing transmission of the electron analyzer as a function of the kinetic energy in order to obtain accurate relative intensity information about the various lines at different kinetic energies. For this purpose Kr $3d$ photoelectron lines and the subsequent $M_{4,5}N_{2,3}N_{2,3}$ Auger lines were recorded. Photoelectron lines move linearly in kinetic energy when varying the photon energy, and their intensities reflect the changing transmission, whereas the kinetic energies, and thus the contribution from the analyzer transmission, of the Auger lines remain fixed. From the relative intensities between the photoelectron and the corresponding Auger spectra the transmission function of an electron analyzer can be determined [15]. The measured PES of RbBr were then normalized using the obtained transmission function.

III. RESULTS AND DISCUSSION

The experimental valence photoelectron spectrum of RbBr (taken from Ref. [8]) is shown in Fig. 1. All the most prominent features are labeled according to the leading atomic contribution to the molecular state obtained from Mulliken population analysis [16–19] for the calculated spectrum. The

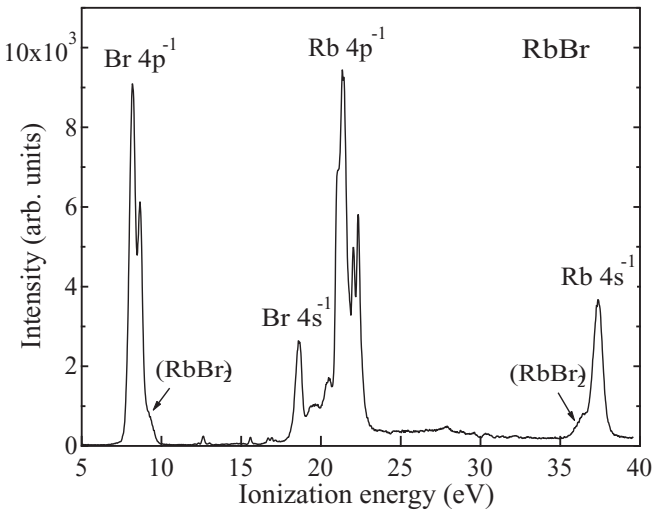

FIG. 1. Experimental valence photoelectron spectrum of RbBr measured with 115 eV photon energy.

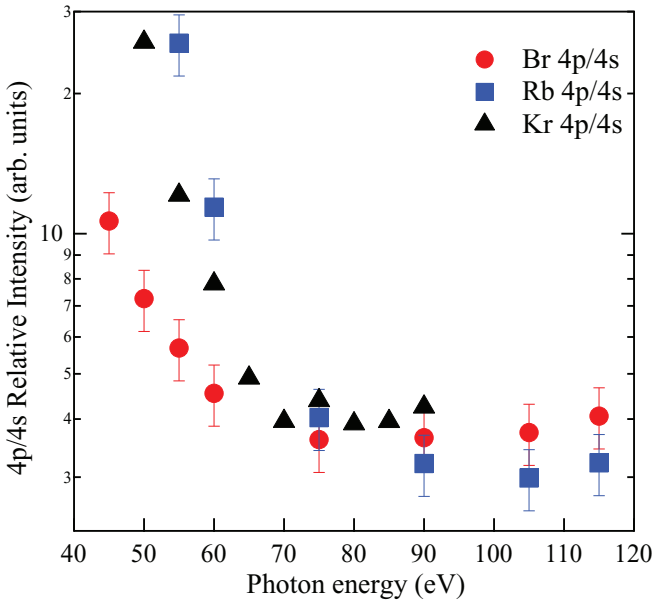

FIG. 2. (Color online) The $4p/4s$ intensity ratios of RbBr and Kr [20,21] as a function of photon energy.

four groups of spectral features assigned to Br $4p^{-1}$, Br $4s^{-1}$, Rb $4p^{-1}$, and Rb $4s^{-1}$ can be found in the ionization energy region between 5 and 45 eV [8].

Figure 2 shows the intensity ratio $4p/4s$ of spectral features for molecular Br and Rb in comparison to atomic Kr. The fairly good overall agreement indicates the similarities in the behavior of state-selective PCS of Rb^+, Br^-, and Kr. The state-selective PCS for $4p$ and $4s$ orbitals in atomic Kr were taken from Refs. [20,21]. The Kr $4p$ PCS decreases from the ionization threshold rapidly, whereas the $4s$ cross section experiences a minimum at about 45 eV photon energy. This is a minimum separating excitation energies where strong electron correlations are the origin of the $4s$ electron emission from an excitation energy range, where the cross sections can be described by a Hartree-Fock-like model with configuration interaction. A more comprehensive review of the photoionization of rare gas atoms using monochromatized synchrotron radiation is given in Ref. [22].

The slope of the Rb $4p/4s$ ratio (Fig. 2) is very much the same as that of Kr on the lower-photon-energy side, whereas the Br $4p/4s$ ratio is clearly lower. At higher photon energies, the Rb $4p/4s$ ratio is smaller than the Br $4p/4s$ ratio; however, here the values overlap within the error limits.

In order to explain where the difference in the behavior of the $4p/4s$ ratios for Rb and Br could originate from, we estimated the behavior of the state-selective PCS as follows: we assumed a fully ionic behavior for both the Br^- and Rb^+ ions similar to that of isoelectronic Kr. Then we accounted for the orbital mixing obtained from the calculations of RbBr ionization.

According to calculations [8], Br $4s^{-1}$ is not a pure state but has a clear Rb $4p^{-1}$ contribution. This increases the Br $4s$ cross section and thus decreases the Br $4p/4s$ ratio; at the lower photon energy where the Rb $4p$ photoionization strength is very high, the resulting Br $4p/4s$ ratio is quite suppressed, as seen in Fig. 2. Rb $4p$ is not a pure state either, but as the $4p$

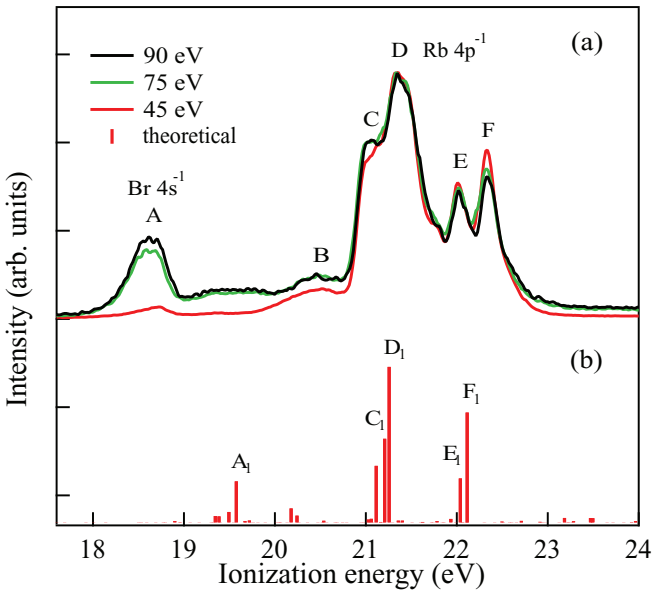

FIG. 3. (Color online) (a) Experimental inner-valence photoelectron spectra of RbBr measured with 45, 75, and 90 eV photon energies. (b) Theoretical spectrum, taken from Ref. [7], presented with vertical red bars.

photoionization strength is an order of magnitude higher than the Br $4s$ photoionization strength, the Rb $4p$ photoionization is hardly affected, and the slope of the Rb $4p/4s$ ratio remains about the same as the corresponding ratio in Kr.

If the dipole matrix elements of Br^-, Rb^+, and Kr were the same, the Rb $4p$ contribution in the Br $4s$ state would decrease the Br $4p/4s$ ratio as detected experimentally (Fig. 2). The contribution cannot be added or subtracted directly, however, as the signs of matrix elements and eigenvectors also play a role. Due to differences in the ionization thresholds of Br^-, Rb^+, and Kr the cross sections may also be shifted even if the ionization strengths are similar.

In addition, the $4s$ cross section of Kr, for instance, is known to display strong many-electron effects. The role of the channel interaction [4] is strong below the minimum of the PCS feeding the weak $4s$ cross section. Furthermore, mixing of $4s^{-1}$ and $4p^{-2}ns/md$ configurations needs to be accounted for when the PCS is described by a Hartree-Fock-like model which predicts well the behavior of the PCS above the minimum. For this reason, it is impossible to accurately determine the amount of the decrease in the Br $4p/4s$ ratio even if the mixing of Br $4s^{-1}$ and Rb $4p^{-1}$ states is predicted by calculations.

The mixing of Br $4s^{-1}$ and Rb $4p^{-1}$ states predicted by theory can be verified in our experiment as follows. The experimental inner-valence PES of RbBr at the energy range of 17–24 eV measured with 45, 75, and 90 eV photon energies are presented in Fig. 3(a). All the most prominent features are labeled with capital letters and are normalized to the D line for better visual presentation of the relative intensity distribution. The D line represents a pure Rb $4p^{-1}$ state based on calculations [8]. Peak A originates mainly from ionization of the Br $4s$ orbital, while peaks C, D, E, and F exhibit mainly Rb $4p$ character. Peak B arises from the dimer $(RbBr)_2$ contribution and configuration interaction satellites of Br $4s^{-1}$. As seen from Fig. 3(a), a drop in the intensity of peak A is followed by a state-selective redistribution of the intensities of peaks C and F, which indicates a mixing of Br $4s^{-1}$ and Rb $4p^{-1}$ states, as predicted by calculations.

Energy splitting of Rb $4p^{-1}$ peaks labeled by C, D, E, and F in the experimental spectrum [Fig. 3(a)] is somewhat underestimated by theory, but the structures labeled C_1, D_1, E_1, and F_1 in Fig. 3(b) are quite well predicted. Mulliken population analysis performed on the calculated Rb $4p^{-1}$ peak manyfold indicates about 15% of the atomic Br $4s^{-1}$ contribution to the C_1 and F_1 lines, while the strongest line, D_1, remains purely Rb character. The theory underestimates the energy separation of the Br $4s^{-1}$ [labeled by A_1 in Fig. 3(b)] and the Rb $4p^{-1}$ peaks. This is most likely related to the many-electron character of the Br $4s^{-1}$ state, which is analogous to photoionization of the atomic Kr $4s^{-1}$ state. In addition to the main Kr $4s^{-1}$ spectral line, a very clear Rydberg series of nd correlation satellites was observed in the Kr photoelectron spectra [4,23]. The satellite structures, which can be observed in the valence photoelectron spectrum of RbBr (Fig. 1) in the ionization energy region of 24–35 eV, were not fully accounted for in the calculations [8].

The many-electron states act as a bridge, allowing strong mixing of the Br $4s^{-1}$ and Rb $4p^{-1}$ states. The mixing creates five prominent peaks in the Rb $4p^{-1}$ region and further has an effect on the behavior of the PCS and branching ratios, as seen in the experiment [Fig. 3(a)].

IV. CONCLUSIONS

In this work we have shown that the behavior of atomic experimental photoionization cross sections of noble gases is similar to that of the photoionization cross sections of the isoelectronic molecules with an ionic type of bonding. The findings indicate that the dipole matrix elements of the isoelectronic atoms could be helpful in developing computational tools for molecular intensity calculations. The experimentally observed branching ratios of valence photoelectron lines in the inner-valence region for the different photon energies are fairly well reproduced by the calculated mixing of molecular Br $4s^{-1}$ and Rb $4p^{-1}$ states.

ACKNOWLEDGMENTS

This work was supported by the Research Council for the Natural Sciences and Engineering of the Academy of Finland. The staff of MAX-lab is acknowledged for providing the facility and beam line for our use and for their contribution during the experiments.

[1] J. Tulkki, S. Aksela, H. Aksela, E. Shigemasa, A. Yagishita, and Y. Furusawa, Phys. Rev. A **45**, 4640 (1992).

[2] S. Aksela, H. Aksela, M. Levasalmi, K. H. Tan, and G. M. Bancroft, Phys. Rev. A **36**, 3449 (1987).

[3] S. Alitalo, A. Kivimäki, T. Matila, K. Vaarala, H. Aksela, and S. Aksela, J. Electron Spectrosc. Relat. Phenom. **114–116**, 141 (2001).
[4] A. Caló, S. Atanassova, R. Sankari, A. Kivimäki, H. Aksela, and S. Aksela, J. Phys. B **39**, 4169 (2006).
[5] S. Benzaid, M. O. Krause, A. Menzel, and C. D. Caldwell, Phys. Rev. A **57**, 4420 (1998).
[6] D. Lin and H. P. Saha, Phys. Rev. A **59**, 3614 (1999).
[7] A. Karpenko, D. Iablonskyi, and H. Aksela, J. Chem. Phys. **138**, 164315 (2013).
[8] A. Karpenko, D. Iablonskyi, S. Urpelainen, J. A. Kettunen, W. Cao, M. Huttula, and H. Aksela, J. Chem. Phys. **140**, 204321 (2014).
[9] J. Schirmer, A. B. Trofimov, and G. Stelter, J. Chem. Phys. **109**, 4734 (1998).
[10] M. Pernpointner, J. Chem. Phys. **121**, 8782 (2004).
[11] DIRAC, a relativistic *ab initio* electronic structure program, release DIRAC10 (2010), written by T. Saue, L. Visscher, and H. J. Aa. Jensen, with contributions from R. Bast *et al.*; see http://dirac.chem.vu.nl.
[12] M. Bassler, A. Ausmees, M. Jurvansuu, R. Feifel, J. O. Forsell, P. de Tarso Fonseca, A. Kivimäki, S. Sundin, S. L. Sorensen, R. Nyholm, O. Björneholm, S. Aksela, and S. Svensson, Nucl. Instrum. Methods Phys. Res., Sect. A **469**, 382 (2001).
[13] A. Mäkinen, M.S. thesis, University of Oulu, 2006.
[14] E. B. Saloman, J. Phys. Chem. Ref. Data **36**, 215 (2007).
[15] J. Jauhiainen, A. Ausmees, A. Kivimäki, S. J. Osborne, A. Naves de Brito, S. Aksela, S. Svensson, and H. Aksela, J. Electron Spectrosc. Relat. Phenom. **69**, 181 (1994).
[16] R. S. Mulliken, J. Chem. Phys. **23**, 1833 (1955).
[17] R. S. Mulliken, J. Chem. Phys. **23**, 1841 (1955).
[18] R. S. Mulliken, J. Chem. Phys. **23**, 2338 (1955).
[19] J. Pipek and P. Z. Mezey, J. Chem. Phys. **90**, 4916 (1989).
[20] J. A. R. Samson and W. C. Stolte, J. Electron Spectrosc. Relat. Phenom. **123**, 265 (2002).
[21] A. Ehresmann, F. Vollweiler, H. Schmoranzer, V. L. Sukhorukov, B. M. Lagutin, I. D. Petrov, G. Mentzel, and K.-H. Schartner, J. Phys. B **27**, 1489 (1994).
[22] J. Schmidt, Rep. Prog. Phys. **55**, 1483 (1992).
[23] S. Svensson, B. Eriksson, N. Mårtensson, G. Wendin, and U. Gelius, J. Electron Spectrosc. Relat. Phenom. **47**, 327 (1988).